Supporting information for:

Free Volume Theory of Hydrocarbon Mixture Transport in Nanoporous Materials

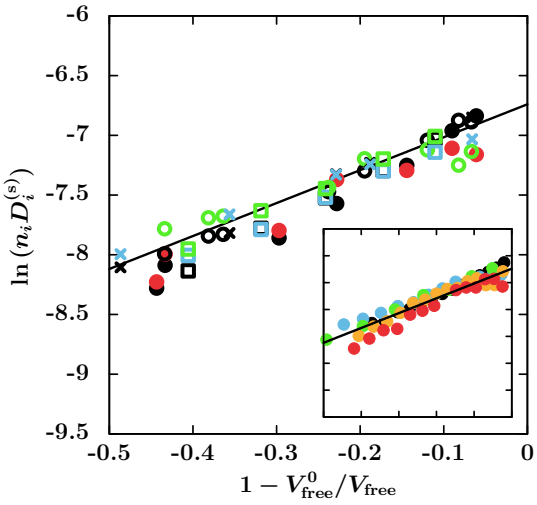

Figure S1: Logarithm of the rescaled self diffusion coefficients $n_i D_i^{(s)}$, with the alkane lenght n_i, versus the free volume fraction V_{free}/V_{free}^0. The latter is calculated independently for a given adsorbed amount Γ. Symbols denote different mixtures: methane/dodecane (dots), methane/hexane (circles), methane/propane (crosses) and methane/propane/hexane (squares). The colors indicate the alkane type: methane (black), propane (blue), hexane (green) and dodecane (red). The solid line is the prediction of the free volume theory $\ln(n_i D^{(s)}) \propto 1 - V_{free}^0/V_{free}$ taken from the single component case (inset where closed symbols are for pure alkanes: methane (black), propane (blue), hexane (green), nonane (orange), and dodecane (red), the solid line is a linear fit).

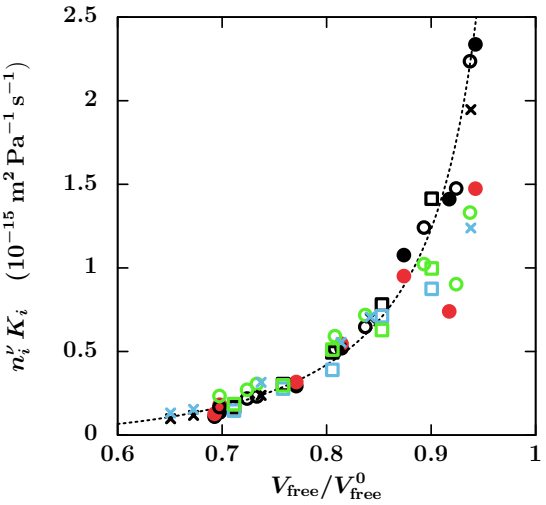

Figure S2: Rescaled permeability $n_i^\nu K_i$, using the correction inspired by the Zimm theory (see text), of the different components in different mixtures as a function of the free volume fraction $V_{\mathrm{free}}/V_{\mathrm{free}}^0$ (with $\nu = 0.7$). The dashed line is a fit using eq 13 (see article) rewritten as $n_i^\nu K_i = K_0/(1 - V_{\mathrm{free}}/V_{\mathrm{free}}^0) \times \exp\left(-\alpha V_{\mathrm{free}}^0/V_{\mathrm{free}}\right)$ with $\alpha = 2.76$, $K_0 = 4.97\ 10^{-15}\ \mathrm{m^2\,Pa^{-1}\,s^{-1}}$ and using $V_{\mathrm{free}}/V_{\mathrm{free}}^0 = 1 - \beta\Gamma$ ($\beta = 0.37$, Fig. S3). Same color code as in Figure S1 is used.

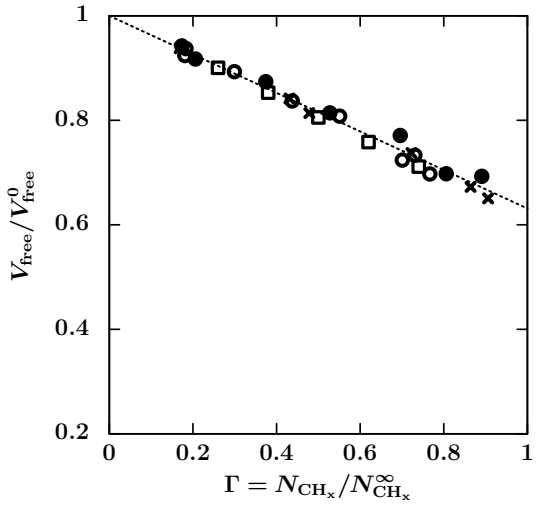

Figure S3: Free volume fraction $V_{\mathrm{free}}/V_{\mathrm{free}}^0$ versus the loading $\Gamma = N_{\mathrm{CH_x}}/N_{\mathrm{CH_x}}^\infty$ for different mixtures (dots: methane/dodecane, crosses: methane/propane, circles: methane/hexane, squares: methane/propane/hexane). The dashed line is a linear fit such as $V_{\mathrm{free}}/V_{\mathrm{free}}^0 = 1 - \beta\Gamma$ with $\beta = 0.37$ (same value as for the pure component case).

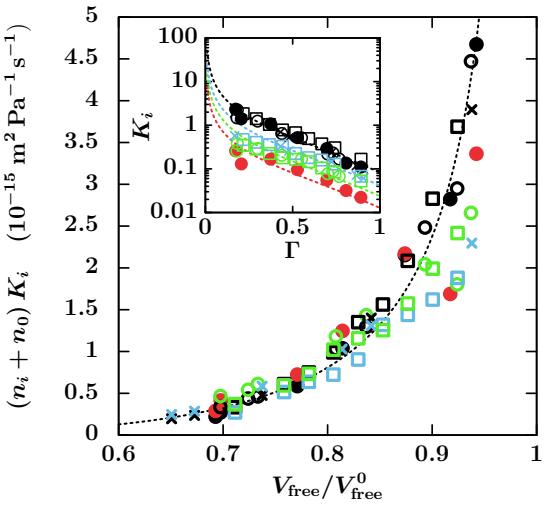

Figure S4: Rescaled permeability $(n_i+n_0)K_i$ of the different components in different mixtures as a function of the free volume fraction $V_{\mathrm{free}}/V^0_{\mathrm{free}}$. The dashed line is a fit using the free volume scaling eq 13 (see article) rewritten as $(n_i + n_0)K_i = K_0/(1 - V_{\mathrm{free}}/V^0_{\mathrm{free}}) \times \exp\left(-\alpha V^0_{\mathrm{free}}/V_{\mathrm{free}}\right)$ with $\alpha = 2.76$, $K_0 = 4.97\ 10^{-15}\ \mathrm{m^2\,Pa^{-1}\,s^{-1}}$ and using $V_{\mathrm{free}}/V^0_{\mathrm{free}} = 1-\beta\Gamma$ ($\beta = 0.37$, Fig. S3). Inset : Permeances K_i in a logscale versus the loading Γ. The dashed lines correspond to the free volume predictions for the different alkanes. Same color code as in Figure S1 is used.

Molecular models

Nanoporous carbon material

The numerical model of nanoporous structure used in this study is taken from the work of Bousige *et al.*[1] The sample is constructed numerically with a Hybrid Reverse Monte Carlo method to fit experimental data such as diffraction data, composition, density.[2,3] In particular, the structure is an atomistic pyrobitumen model containing 5410 atoms in a 5 nm cubic box characterized by a mass density of 0.8 $\mathrm{g\,cm^{-3}}$ and a porosity about 0.56. The structure, which is analogous to a very mature kerogen (pore size, density, chemical composition and hybridization ratio, morphological disorder),[2,4–6] is mainly composed of carbon atoms but also of hydrogen atoms (hydrogen index H/C = 0.091) and oxygen atoms (oxygen index O/C = 0.0087). The structure is isotropic and characterized by pore sizes ranging from 3 to 15 nm. Adsorption isoterms for different linear alkanes are shown in Fig. 1 together with a snapshot of a ternary mixture of methane, propane and hexane adsorbed in the nanoporous structure.

n-alkanes model

For the fluids, we use a well established united atoms force field for alkanes.[7] A coarse grained approach is used in which each functional group CH_x is represented by a single interaction site (where $x = 2$ or 3 depending on the position of the group in the alkyl chain). The pseudo atoms of one n-alkane molecule are connected as a flexible chain with bonds of a fixed length (1.54 Å). Bending and torsion of the chain are described by intramolecular interaction potentials thus constraining the angles between three neighboring atoms (θ) and the dihedral angles formed by four neighboring atoms (ψ). The bending potential is a harmonic potential:

$$U_{\mathrm{bending}}(\theta) = \frac{C}{2}(\theta - \theta_0)^2 \tag{1}$$

with $C/k_B = 62500\,K$ and $\theta_0 = 114\,^\circ$. The torsion potential is given by:

$$U_{\text{torsion}}(\psi) = C_1[1 + \cos(\psi)] + C_2[1 - \cos(2\psi)] + C_3[1 + \cos(3\psi)] \tag{2}$$

with $C_1/k_B = 355.03\,K$, $C_2/k_B = -68.19\,K$ and $C_3/k_B = 791.32\,K$. Liquid-solid and liquid-liquid interactions (also for functionnal sites of the same molecule separated by at least four neighbors) are modeled by the Lennard-Jones (LJ) potential

$$U_{\text{LJ}}(r_{ij}) = 4\epsilon_{ij}\left[\left(\frac{\sigma_{ij}}{r_{ij}}\right)^{12} - \left(\frac{\sigma_{ij}}{r_{ij}}\right)^{6}\right] \tag{3}$$

as a function of $r_{ij} = |\boldsymbol{r_i} - \boldsymbol{r_j}|$ the distance between the centers of the interacting atoms. We use the Lorentz-Berthelot mixing rules to compute the parameters $\epsilon_{ij} = \sqrt{\epsilon_i \epsilon_j}$ and $\sigma_{ij} = (\sigma_i + \sigma_j)/2$ as a function of the interacion strength ϵ_i and the group diameter σ_i (given in Tab. S5). The atoms of the structure are frozen during all the simulations performed in this work so that the swelling and flexibility effects are not investigated here. Even if this effect can increase the transport properties, we do not expect significant changes since the structure of the matrix is mainly composed of graphitic domains and is thus rigid.[1]

Site	$\epsilon/k_B\,(K)$	$\sigma\,(\text{Å})$
C	28	3.36
H	15	2.42
O	78	3.17
CH_2	46	3.95
CH_3	98	3.75
CH_4	148	3.73

Figure S5: Lennard-Jones parameters used in the simulations for the atoms of the structure (C, H, O) and the functionnal sites of the fluid molecules (CH_x).

Numerical methods

Configurational Biased Grand Canonical Monte Carlo simulations (CBGCMC)

We use the Grand Canonical Monte Carlo scheme described in[8,9] with a biased procedure to simulate adsorption in the grand canonical (μVT) ensemble. Monte Carlo simulation steps consist of insertion, deletion, partial regrowth, translation or rotation of the alkane chains. Since we deal with long and flexible molecules in a very confining host matrix, we use a biased technique for the insertion and partial regrowth to increase the probability to find energetically favorable configurations. This technique allows us to control the composition and the total loading of the adsorbed fluids.

Equilibrium Molecular Dynamics (EMD)

We consider mixtures of hydrocarbons composed of ℓ different types of n-alkanes at a molecular density $\rho = N/V$ with molecular fractions $x_i = N_i/N$, with N_i the number of molecules of component i and N the total number of molecules in the mixture ($\sum_{i=1}^{\ell} x_i = 1$). We define for a component i, its monomer length n_i, its number density $\rho_i = N_i/V$, its chemical potential μ_i and its centre of mass velocity:

$$\boldsymbol{v_i} = \sum_{k=1}^{N_i} \boldsymbol{v_i^k}/N_i \tag{4}$$

with $\boldsymbol{v_i^k}$ the velocity of the k^{th} molecule of the component i.

In order to perform Equilibrium (EMD) or Non Equilibrium (NEMD) simulations of the systems considered here, we use MD simulations in the NVT ensemble with the LAMMPS software.[10] We use a 1 fs time step to integrate the equations of motion over 10 ns long simulation runs (40 for some low loading systems), where the initial configurations at different loadings and compositions are prepared using the CBGCMC technique. We investigate

several binary mixtures and a ternary case. In all the simulations, the temperature is kept constant at 423 K by the use of a Nosé-Hoover thermostat with a relaxation time of 0.1 ps. During NEMD, no thermostat is applied in the flowing direction, although it does not affect the temperature of the system. Transport coefficients at equilibrium are computed by integrating the velocity auto correlation functions:

$$D_i^{(\mathrm{c})} = \frac{N_i}{3} \int_0^\infty \langle \boldsymbol{v_i}(t) \cdot \boldsymbol{v_i}(0) \rangle_{\mathrm{eq}} \, \mathrm{d}t \tag{5}$$

for the collective diffusivities, and

$$D_i^{(\mathrm{s})} = \frac{1}{3N_i} \sum_{k=1}^{N_i} \int_0^\infty \langle \boldsymbol{v_i^k}(t) \cdot \boldsymbol{v_i^k}(0) \rangle_{\mathrm{eq}} \, \mathrm{d}t \tag{6}$$

for the self diffusivities. Inserting eq 4 in eq 5 straightforwardly leads to the following relations between the collective and the self diffusion coefficients:

$$D_i^{(\mathrm{c})} = D_i^{(\mathrm{s})} + \frac{1}{3N_i} \sum_{k \neq p}^{N_i} \int_0^\infty \langle \boldsymbol{v_i^k}(t) \cdot \boldsymbol{v_i^p}(0) \rangle_{\mathrm{eq}} \, \mathrm{d}t \; . \tag{7}$$

Non Equilibrium Molecular Dynamics (NEMD)

Steady state flow of hydrocarbon mixture in the kerogen structure subjected to a pressure gradient $\boldsymbol{\nabla} P$ was investigated using non equilibrium molecular dynamics. Since a pressure gradient corresponds to a force per unit volume $\boldsymbol{F}/V = -\boldsymbol{\nabla} P$ (V is the system volume), a constant force $\boldsymbol{f} = \boldsymbol{F}/N = -\boldsymbol{\nabla} P/\rho$ was applied to each of the N molecules of the confined mixture ($\rho = N/V$ is the mixture number density). The mean fluid flow velocities for each component is obtained using eq 4. Forces are applied on the z direction and the velocities are evaluated in the same direction when steady-state is reached.

Free volume computation

We use a grid based algorithm to determine the porous volume V_{free}^0 of the material as well as the free volume V_{free} still available when a given amount of fluid is adsorbed in the host matrix. At each node of the lattice we check if a pointlike probe lie within an atom of the structure or of the fluid. The atoms in the simulation box are not allowed to move and are considered as hard spheres of diameter σ (see Table S5). The volume of the simulation box times the ratio of the number of free grid nodes to the total number of grid nodes gives the free volume. A lattice spacing of 0.2 nm is found to be sufficient to obtain converged results. Fig. S3 gives the linear evolution of the free volume normalized by the total porous volume as a function of the total monomer loading Γ for all the mixtures considered in the article. It is to be noted that these results are the same as for the pure component case.

Maxwell-Stefan framework

Here we intend to transpose our model to the Maxwell-Stefan (MS) theory which is widely used in chemical engineering.[11–13] We start by introducing the constitutive equations of the MS theory for mixtures:

$$-\frac{\boldsymbol{\nabla}\mu_i}{k_B T} = \sum_{j=1}^{\ell} \frac{x_j(\boldsymbol{v_i} - \boldsymbol{v_j})}{\tilde{D}_{ij}} \,, \tag{8}$$

when the following condition is imposed to the potential gradients :

$$\sum_{i=1}^{\ell} x_i \boldsymbol{\nabla}\mu_i = \mathbf{0} \,. \tag{9}$$

We have used here the so called Maxwell-Stefan diffusivities $\tilde{D}_{ij}$ which can be seen as the inverse of phenomenological friction coefficients between two components. By comparison with the Onsager framework we can relate the MS diffusivities with the Onsager coefficients

; in the binary case we simply have

$$\tilde{D}_{12} = \frac{x_1}{x_2}\Lambda_{22} + \frac{x_2}{x_1}\Lambda_{11} - 2\Lambda_{12} \; . \tag{10}$$

As in the case of the Onsager framework, the cross correlations can be neglected (inset of Fig. S6). This motivates us to use predictive equations solely based on the self diffusion coefficients of the pure components. For binary mixtures, the usual Darken relation

$$\tilde{D}_{12} \simeq x_1 D_2^{(\mathrm{s})} + x_2 D_1^{(\mathrm{s})} \tag{11}$$

holds and can be used to establish a free volume theory for the MS diffusivities as

$$\tilde{D}_{ij} = \frac{k_B T}{n_{ij}\xi_0} \exp\left(-\alpha \frac{V_{\mathrm{mix}}}{V_{\mathrm{free}}}\right) \tag{12}$$

where the parameters α and ξ_0 are also given by the pure component case, with $n_{ij} = n_i n_j/(x_i n_i + x_j n_j)$ as a mixing rule for the alkane length in the binary case. We can extend these relations in the case of arbitrary mixture by the use of the multicomponent Darken equation derived by Liu *et al.*:[14]

$$\tilde{D}_{ij} \simeq D_i^{(\mathrm{s})} D_j^{(\mathrm{s})} \sum_{k=1}^{\ell} \frac{x_k}{D_k^{(\mathrm{s})}} \; , \tag{13}$$

which gives the same result as eq 11 when $\ell = 2$. We can thus generalize the free volume theory (eq 12) for an arbitrary number of components with the following mixing rule:

$$n_{ij} = \frac{n_i n_j}{\sum_{k=1}^{\ell} x_k n_k} \tag{14}$$

The inset of Fig. S6 confirms the validity of the multicomponent Darken equations in our cases, and that the free volume theory can be expressed in the MS framework within a convenient form as for the Onsager framework. As in the Onsager framework, the MS

diffusivities obey the same free volume scaling as in the pure component case where we have used the recent predictive model of Liu *et al.*[14] to obtain a mixing rule for the alkane length.

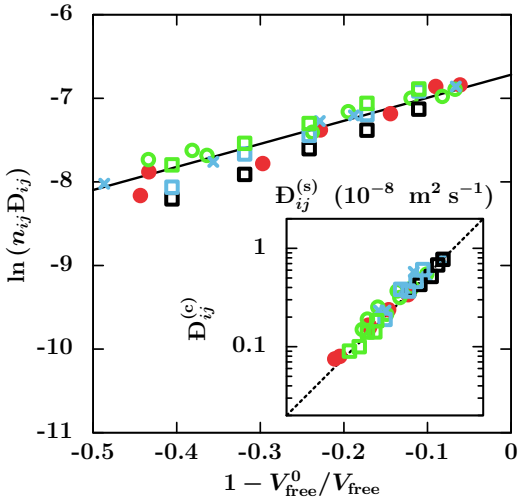

Figure S6: Logarithm of the rescaled MS diffusivities $n_{ij}\tilde{D}_{ij}$ computed exactly from the fluctuations,[14] with $n_{ij} = n_i n_j / \sum_{k=1}^{\ell}(x_k n_k + x_k n_k)$ coming from eq 13, as a function of the free volume term in the same way as Fig. S1. The solid line corresponds to the prediction of the self diffusion coefficient of the pure component case (Inset of Fig. S1). Inset: Comparisons between the MS diffusivities computed exactly and evaluated using eq 13 where the cross correlations are neglected. Blue crosses, green circles and red dots denote respectively methane/propane, methane/hexane and methane/dodecane binary mixtures. For the methane/propane/hexane ternary mixture denoted by the empty squares, green, blue and black correspond to the three different MS diffusivities involving respectively methane and propane, methane and hexane, and propane and hexane.

References

(1) Bousige, C.; Ghimbeu, C. M.; Vix-Guterl, C.; Pomerantz, A. E.; Suleimenova, A.; Vaughan, G.; Garbarino, G.; Feygenson, M.; Wildgruber, C.; Ulm, F.-J.; Pellenq, R. J.-M.; Coasne, B. *Nature Materials* **2016**, *15*, 576–582.

(2) Pikunic, J.; Llewellyn, P.; Pellenq, R.; Gubbins, K. E. *Langmuir* **2005**, *21*, 4431–4440.

(3) Jain, S. K.; Pellenq, R. J.-M.; Pikunic, J. P.; Gubbins, K. E. *Langmuir* **2006**, *22*, 9942–9948.

(4) Firouzi, M.; Rupp, E. C.; Liu, C. W.; Wilcox, J. *International Journal of Coal Geology* **2014**, *121*, 123–128.

(5) Orendt, A. M.; Pimienta, I. S.; Badu, S. R.; Solum, M. S.; Pugmire, R. J.; Facelli, J. C.; Locke, D. R.; Chapman, K. W.; Chupas, P. J.; Winans, R. E. *Energy & Fuels* **2013**, *27*, 702–710.

(6) Kelemen, S. R.; Afeworki, M.; Gorbaty, M. L.; Sansone, M.; Kwiatek, P. J.; Walters, C. C.; Freund, H.; Siskin, M.; Bence, A. E.; Curry, D. J.; Solum, M.; Pugmire, R. J.; Vandenbroucke, M.; Leblond, M.; Behar, F. *Energy & Fuels* **2007**, *21*, 1548–1561.

(7) Martin, M. G.; Siepmann, J. I. *The Journal of Physical Chemistry B* **1998**, *102*, 2569–2577.

(8) Smit, B. *Molecular Physics* **1995**, *85*, 153–172.

(9) Falk, K.; Pellenq, R.; Ulm, F. J.; Coasne, B. *Energy & Fuels* **2015**, *29*, 7889–7896.

(10) Plimpton, S. *Journal of Computational Physics* **1995**, *117*, 1–19.

(11) Krishna, R.; Paschek, D. *Separation and Purification Technology* **2000**, *21*, 111–136.

(12) Krishna, R. *Microporous and Mesoporous Materials* **2014**, *185*, 30–50.

(13) Arnošt, D.; Schneider, P. *The Chemical Engineering Journal and the Biochemical Engineering Journal* **1995**, *57*, 91–99.

(14) Liu, X.; Vlugt, T. J.; Bardow, A. *Industrial & Engineering Chemistry Research* **2011**, *50*, 10350–10358.